Investigating the feasibility of space-to-ground laser communications in Singapore's weather

By S N Kylash[1], Varadharajan Harish[1], Siddhaarth Dharani[1], Yuen Xianghao[1], Seow Yongli[1], Wong Wei Xiang Kendrick[2]

[1] *NUS High School of Mathematics and Science*
20 Clementi Ave 1, Singapore 129957
[2] *DSO National Laboratories,*
12 Science Park Dr, Singapore 118225

Abstract

In this paper, we investigate the feasibility of laser communications in Singapore's weather conditions. Solar and lunar spectra were observed with a Silicon spectrometer in the ranges of 600nm-1100nm under various cloud conditions. We then categorised this data by the weather condition (cloudy and clear sky), and compared cloudy sky data to clear sky data to see if any specific wavelengths are absorbed preferentially. Using attenuation coefficients from literature and comparing it with cloud cover data from the satellite Himawari-9, we calculated the total attenuation caused by the clouds. Our analysis combined with the Himawari-9 data was unreliable and we deemed it was because Himawari-9 was not precise enough to accurately determine the sky condition in our exact observation area. In the end, we did a subjective analysis of our data based on our subjective classification of the cloud cover. We managed to show that clouds don't have absorption lines for the wavelengths between 600nm-1000nm. However, we could not show a correlation between satellite cloud cover and attenuation. This study could be improved further with a spectrometer made of a different material and more accurate satellite data.

Introduction

Space-to-ground communications are extremely important in today's world as they enable information to be transmitted over vast distances across the globe. This enables services like long-distance phone calls or GPS systems to function. Space-to-ground communication occurs when data is transmitted from a satellite in space to a ground station on Earth. Radio waves have long been used for this process with remarkable success such as 4G which has data transmission rates of 100MBps[1]. However, a drawback of using radio waves is that they have frequencies in the GHz range, which means they have a low bandwidth, thus resulting in the rate of data transfer limited to about 1GBps[2]. Thus, to increase the rate of data transfer, lasers are an option. Lasers have frequencies in the hundreds of THz range, and can hence transfer up to 200GBps[2]. They are also far more secure than radio as the indirect signal from an outside observer has a high enough signal-to-noise ratio, making it undecodable[3]. However, unlike radio waves, lasers are more susceptible to attenuation caused by clouds in the sky, due to their higher frequencies and Mie scattering[4]. The dominant scattering process in the atmosphere is Rayleigh scattering, whose effect is inversely proportional to the fourth power of the wavelength of the electromagnetic wave[4]. As a result, lasers which have wavelengths in the nanometer range are scattered much more than radio waves, which have wavelengths several meters long. The scattered photons are deflected away from their original path. Thus, the strength of the signal received at the target location is greatly diminished.

Previous work has been done to calculate the attenuation of the atmosphere for lasers in the near infrared range during clear skies[5]. However, Singapore is situated in a climatically volatile region and does not consistently experience clear atmospheric conditions. Therefore, we wanted to investigate this attenuation in the context of Singapore's weather. We aimed to find out how characteristics of Singapore's weather, such as the cloud density, affect the attenuation of the laser. We intend on doing this by collecting the spectrum of the object under cloud cover and comparing it with the spectrum obtained when there are no clouds. These include the position of the object in the sky relative to us, as well as the density and thickness of the clouds. Using that, we will investigate what percentage of the signal is scattered and investigate characteristics of this scattering, such as whether certain wavelengths of light are scattered more than others. Then we will use this to characterize the impact of weather on optical transmission. Using our results, we will determine the feasibility of laser communication in Singaporean weather and sky conditions.

Methodology

To obtain spectrum data of celestial objects, we used a spectrometer from StellarNet connected to a telescope via an optic fiber cable. The telescope we used was a Celestron NexStar 5-SE telescope with a computerized mount capable of automatically tracking the object's trajectory in the sky. The spectrometer comes with a software (SpectraWiz) that can be installed on our laptops. This software allowed us to capture the moon's spectrum and save it for data analysis. The steps we took were as follows:

1. Set up the telescope and activate the auto tracking such that it is pointing at the object to be tracked and following its trajectory across the sky.

2. Connect the spectrometer to the telescope via the optical fiber cable. Unlike conventional optical fiber cables, one end of our fiber cable is a hexagonal bundle of 7 cables. This maximises the light gathering power of the fiber. This bundle is rearranged into a line at the other end of the fiber cable so that the light can be aligned with the thin rectangular slit of the spectrometer and enter it to be analysed. Hence, it was important to make sure the fiber cable was aligned with the slit inside the spectrometer, so we rotated the fiber cable until a maximum was reached in the observed spectrum.

3. Take a dark reading by covering the telescope, and saving the noise observed after taking a dark reading. Taking a dark reading eliminates any systematic error that may be present in the detector and allows us to get a base line for the stochastic noise caused by electrons entering the spectrometer even in dark conditions. The background noise was taken to account for the stochastic noise.

4. Take spectrum readings during the following conditions:

   (a) Minimal-to-no clouds: The object is clearly visible in the sky, and the surrounding area is clear.

   (b) Light clouds: The object is shrouded my mostly transparent clouds, and the surrounding area is mostly clear.

   (c) Medium clouds: The object appears fuzzy, and the surrounding area is cloudy.

   (d) Heavy/dense clouds: The object is mostly-to-fully shrouded in clouds and is hardly visible, if at all.

Figure 1: Sample Observed Cloud Conditions

The pictures above represent (in sequential order): light clouds, medium clouds, no clouds and dense clouds.

We collected the spectrum data of the object by observing it through the telescope. For this project, the objects we chose to observe were the moon and the sun. These objects were chosen due to their large angular size and well-documented spectrum[6]. To ensure our results were consistent, we only made moon observations on the weeks when there were full moons. In particular, the full moon weeks from August through November were when we recorded spectrum data.

The readings we obtained from the StellarNet spectrometer were read and analysed by a Python program made by us. Firstly, we took the intensity of each data point and multiplied by the attenuation multiplier that follows from the Beer-Lambert law:

$$I = I_0 \cdot e^{-\mu x}$$

Where μ is the attenuation coefficient in km^{-1} and x is the distance travelled by the light from the moon to the telescope in km. This multiplier would then be applied to every data point. To find it, we used the atmospheric height and multiplied it with the relative airmass, which is a trigonometric function of the angle that the moon makes with the zenith θ. To be precise, the relative airmass is given by $\sec(\theta)$. Refer to Figure 2 below for a visual representation of the calculation for the relative airmass, where Y is the distance the light travels through and X is the atmospheric height:

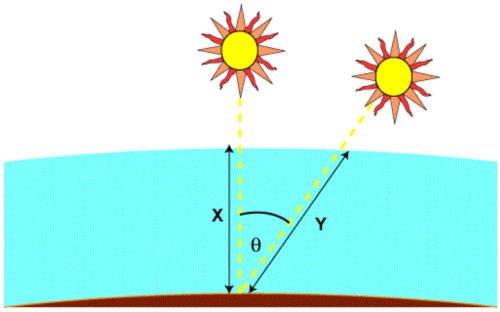

Figure 2: A visual representation of the calculation for the relative airmass

The attenuation coefficients we obtained from *Elterman, L.* (1963)[7] were calculated in units $dB \cdot km^{-1}$ (denoted as λ). In order to convert it to a linear attenuation coefficient, we applied the following formula:

$$\mu = ln10 \cdot \frac{\lambda}{10x}$$

Where x is the same as above. After obtaining μ, we plugged it into the Beer-Lambert law to obtain the attenuation multiplier of light ($e^{-\mu x}$).

Moreover, when making the corrected curve, the program also accounts for atmospheric attenuation by getting airmass data from a planetarium software called Stellarium, and the attenuation coefficients from *Elterman, L.* (1963)[7]. Since the coefficients given in the paper were at distinct wavelength values from 400-4000nm, we approximated a continuous function for the attenuation coefficients from 600-1100nm. The regression function we used was:

$$\hat{y} = \frac{1}{a(\hat{x})^4} + b$$

and the regression coefficients we used were $a = 1.6187 \times 10^{-10}$ and $b = 0.112267$. We also assumed the effective atmospheric height to be 18km. Since about 80% of the atmosphere's mass and 99% of its water vapour is in the troposphere[8], we can neglect the other layers of the atmosphere. As a result, we will regard the atmospheric height from Figure 2 as the tropospheric height, which has been determined to be about 18km[8] in the tropical area where Singapore is located.

As mentioned above, the airmass gives us a measure of how far the light traverses through the atmosphere before reaching the spectrometer and the attenuation coefficient allows us to calculate the total decrease in intensity of the light. The Stellarium software was also used to get the altitude and azimuth of the object we are looking at for our analysis with Himawari-9 data.

Since the spectrometer has Silicon detectors, it has varying sensitivities to different wavelengths of light. For instance, the spectrometer is much less sensitive to light of 1000nm than to light of 700nm. To characterise this, we shone a standard white light source with a known spectrum into the telescope, which was connected to the spectrometer by the optic fiber cable. We then recorded the observed spectrum. We plotted this as our calibration graph for the spectrometer for the wavelength regions 600nm – 1100nm. Error bars were included at regular intervals in red

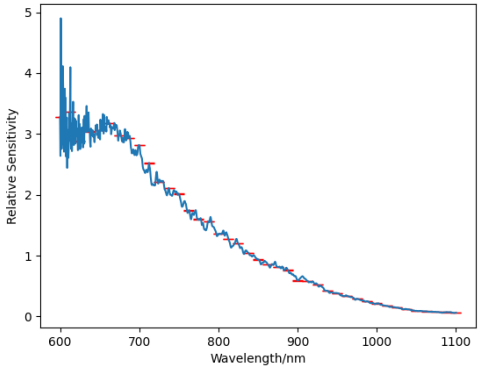

Figure 3: Spectrometer response curve

Once this was known, we divided each dataset in the observed spectrum by the datapoint of our calibration curve at the corresponding wavelength of the dataset which allowed us to correct for silicon's sensitivity. These corrections of atmospheric attenuation and our silicon detector allow us to compare data from different times and different days against each other so that any significant changes in the observed spectrum can be attributed solely to the cloud cover.

The python program we used first calculates the amount of error for each respective day by analysing the noise data we had obtained. Then, it extracts the data and corrects it using the silicon curve and atmospheric attenuation mentioned above to obtain a curve, which is saved as a data file and graph. It then compares every graph to the "normal" graph (least cloud cover). To do so, it gets the amount of attenuation across all wavelengths and saves this as the scale factor to be used later with satellite data. Then both graphs are normalised to see if any particular wavelengths are absorbed more than others.

In addition, we were also able to obtain data from the geostationary meteorology satellite Himawari-9 on the level of cloud cover during the time of observation. Himawari-9 is a satellite that detects radiation from the earth in many different wavelengths. In *B. Purbantoro et al.* (2018)[9], it was reported that the temperature difference between BT15 and BT16 was a good indicator of cloud cover where higher temperatures translate to clearer skies. Thus, we found the temperature difference in the patch of sky where the clouds we were observing our object through were at.

Results

Spectrum Analysis

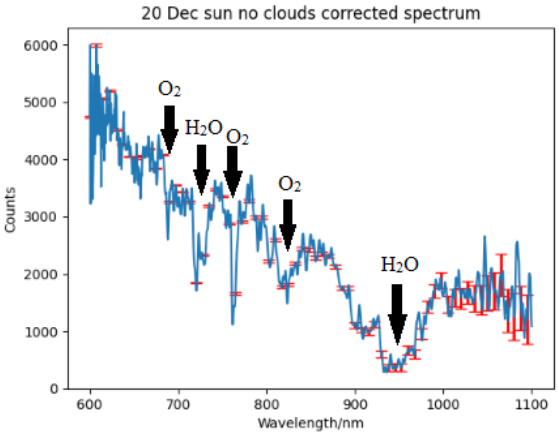

Figure 4: Spectrum of the Sun with no clouds present

Here is the spectrum of the sun with no clouds present after the Silicon curve and atmospheric attenuation. As can be seen there are multiple noticeable dips in the readings which correspond to the absorption lines of various compounds. The drops in readings at around 715nm and at around 940nm are caused by water in the atmosphere[10][11]. The ones at 690nm, 760nm and 810nm correspond to the absorption wavelengths of oxygen in the atmosphere[12]. These are the typical absorption lines after solar radiation passes through our atmosphere and is well documented[6]. We also plotted a graph of the normalised cloudy data divided by the normal for each file. As mentioned above this was done to observe any absorption line specific to clouds and the Mie scattering caused by them.

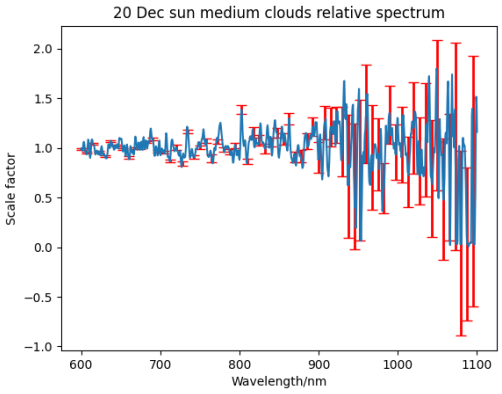

Figure 5: Spectrum of sun with medium clouds divided by normal

Above is the spectrum for a medium clouds reading. Due to the absorption lines of H_2O at 940nm and the low sensitivity of our spectrometer above 1000nm, those readings have quite large error bars due to the high signal to noise ratio. As can be seen there are no visible dips in the data that can't be explained by noise. We believe this shows that clouds don't have additional absorption lines in the 600nm-1000nm range. However, despite the high noise, Mie scattering cannot be observed from our data despite the clouds. We believe that this is due to our equipment not being sensitive enough and the high signal-to-noise ratio. Low integration times were used due to a count limit on our spectrometer. However, this meant that for higher cloud covers we got anywhere from 90%-95% the number of counts a cloudless reading would give. This caused the signal-to-noise ratio for denser cloud covers to be so high as to be unable to observe Mie scattering.

We also overlaid the "normal" graph with the normalised cloudy graph as another visual check to see if some wavelengths are preferentially absorbed over others. Below, in Figure 6, the orange graph is the data under cloud conditions and the blue graph is the "normal", and the cloud density label is very subjective and is based on what we see and the maximum counts observed by the spectrometer. As can been seen from Figure 5 and Figure 6, there are no visible dips in the data that can't be explained by noise. We believe this shows that clouds don't have additional absorption lines in the 600nm-1000nm range.

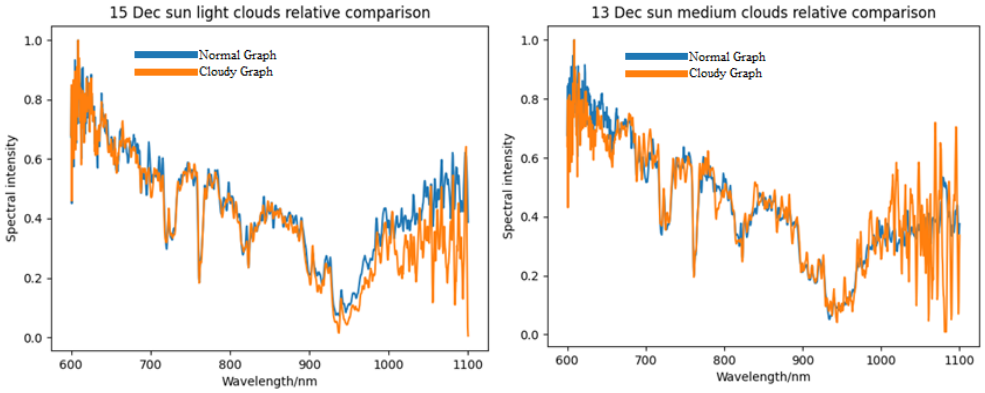

Figure 6: Cloud density vs "Normal" graphs

Analysis with Himawari-9 data

In Figure 7 below, we plotted a graph of the reciprocal of the scale factor against the temperature difference in the patch of sky we observed. As can be seen, there is little, if at all, correlation observed between the scale factor and the temperature difference gathered from the Himawari-9 data.

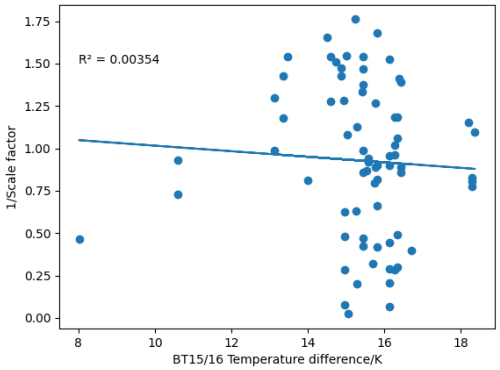

Figure 7: Scale factor against temperature difference

Discussion

For our heavy cloud data, so little light comes through that the noise floor is significant and is magnified by our Silicon curve for higher wavelengths. Thus, the graphs for heavier cloud data may be inaccurate for wavelengths approximately in the range of 1000nm and above. Due to Silicon having very low sensitivity to light above 1000nm, the noise floor and the signal to noise ratio gets magnified by about 17 times and thus is much more inaccurate compared to our no clouds data.

One of the main issues was the equipment we had. Our spectrometer uses Silicon and thus is very insensitive to wavelengths above ∼1000nm. Thus, most of our data is very inaccurate for wavelengths above 1000nm. Moreover, during periods of heavy cloud cover, the error in our readings due to noise was very high due to having to multiply them by a large number in order to normalize them. Thus, our data for 1000nm and up is very inaccurate. Moreover, the satellite we were using, Himawari-9, does not give precise enough data for our purposes. Firstly, the smallest pixel size we could get was a $4km^2$ (2km $\times$ 2km) patch of sky which is much larger that the 0.5° size objects we are looking at. Moreover, Himawari-9 only gives data once every 10 minutes which is not often enough for the purposes of our research. There were many instances of multiple different cloud covers happening in the same 10 min window. While taking measurements, the clouds can move out of the way or move in view during this 10min window. This is why our graph relating the Himawari-9 data doesn't show a clear trend.

In the future, this study could be replicated with a spectrometer made of InGaAs which is more sensitive to wavelengths between 900nm-1700nm[13]. A more accurate spectrometer with a higher count limit would also help reduce the error bars and noise present in our data. A function to predict the percentage signal lost relating to cloud cover would require far more accurate, frequent and precise data than that which is given by Himawari-9.

Conclusion

In this paper we analysed solar and lunar spectra through various weather conditions. We were unable to observe any absorption lines between 600nm-1100nm caused by the clouds in Singapore. Our data for 1000nm-1100nm is too noisy to definitively say that there are no absorption lines. However, there are anomalies in our data such as the lack of evidence of Mie scattering. We have not been able to show a correlation between cloud cover data from Himawari-9 and our scale factor. To prove such a correlation a satellite like the one mentioned is the discussion section would most likely be necessary.

In conclusion, we have shown that for wavelengths between 600 and 1000nm, clouds do not impose additional wavelength restrictions for space-to-ground laser communication as no additional absorption lines were observed during our study. However, wavelengths that are already absorbed in the atmosphere like in Spectrum Analysis should still be avoided. Using wavelengths of 671nm and 850nm like in *SK. Liao et al.* (2017)[14] will result in minimal interference from clouds. However, we have not been able to give a metric to show how much of said signal is lost due to cloud cover. More advanced technologies with far more accurate and precise satellite data would be necessary to further investigate the feasibility of satellite laser communication under local weather conditions.

Acknowledgements

The authors would like to thank Ayesha Reezwana Tumpa from NUS Centre for Quantum Technologies, and her team of researchers from NUS High School of Mathematics and Science, Ng Wei Xiang, Caldras Tan Hong Xun and Lu Yanjie, for guiding us in our analysis and providing us with processed data from the Himawari-9 satellite, as well as Albert Lim from Astro Scientific Centre Pte Ltd for providing us with timely help with equipment we used.

Bibliography

[1] G. S. Nitesh and A. Kakkar. "Generations of mobile communication." In: *IJARCSSE Conference* 32 (2016). URL: https://www.researchgate.net/publication/326462813_Generations_of_Mobile_Communication.

[2] B. S. Robinson et al. "TeraByte InfraRed Delivery (TBIRD): a demonstration of large-volume direct-to-Earth data transfer from low-Earth orbit." In: *Free-Space Laser Communication and Atmospheric Propagation XXX* 10524 (2018). DOI: 10.1117/12.2295023.

[3] Konrad Banaszek et al. "Optimization of intensity-modulation/direct-detection optical key distribution under passive eavesdropping." In: *Opt. Express* 29.26 (2021), pp. 43091–43103. DOI: 10.1364/OE.444340. URL: https://opg.optica.org/oe/abstract.cfm?URI=oe-29-26-43091.

[4] H. Weichel. "Laser Beam Propagation in the Atmosphere." In: *Proceedings of SPIE–the International Society for Optical Engineering* 10319 (1990). URL: https://books.google.com.sg/books?id=OzkZOo5SRj8C&lpg=PP11&ots=I4_YuJXO4Q&dq=laser%20beam%20propagation%20in%20atmosphere&lr&pg=PP11#v=onepage&q=laser%20beam%20propagation%20in%20atmosphere&f=false.

[5] R. A. McClatchey and J. E. Selby. "Atmospheric attenuation of laser radiation from 0.76 to 31.25/um." In: *Environmental Research Paper* 460 (1974). URL: https://www.researchgate.net/publication/326462813_Generations_of_Mobile_Communication.

[6] X. Han et al. "Recent progress in near-infrared light-harvesting nanosystems for photocatalytic applications." In: *Applied Catalysis A: General* 644 (2022). URL: https://www.sciencedirect.com/science/article/pii/S0926860X22003593.

[7] L. Elterman. "A model of a clear standard atmosphere for attenuation in the visible region and infrared windows." In: (1963). URL: https://books.google.com.sg/books?id=d-BBl8V1EFIC&pg=PA2#v=onepage&q&f=false.

[8] "The Earth's Atmosphere". In: *Radio Wave Propagation for Telecommunication Applications*. Springer Berlin Heidelberg, 2005, pp. 13–34. DOI: 10.1007/3-540-26668-2_2. URL: https://doi.org/10.1007/3-540-26668-2_2.

[9] B. Purbantoro et al. "Comparison of Cloud Type Classification with Split Window Algorithm Based on Different Infrared Band Combinations of Himawari-8 Satellite." In: *Advances in Remote Sensing* 7.3 (2018), pp. 218–234. DOI: 10.4236/ars.2018.73015.

[10] crisp.nus.edu.sg. "Absorption by Gaseous Molecules." In: URL: https://crisp.nus.edu.sg/~research/tutorial/absorb.htm#irabs.

[11] C. Starr, C. A. Evers, and L. Starr. "Biology: Concepts and applications." In: (2006). URL: https://archive.org/details/biologyconceptsa06edstar.

[12] A. Blazquez-Castro. "Direct 1O2 optical excitation: A tool for redox biology." In: *Redox biology* 13 (2017), pp. 39–59. DOI: 10.1016/j.redox.2017.05.011.

[13] Semih YURTSEVEN et al. "Investigation of Enviromental Effects on the Normalized Spectral Responsivity of an InGaAs Detector". In: *2019 IEEE International Symposium on Medical Measurements and Applications (MeMeA)*. 2019, pp. 1–6. DOI: 10.1109/MeMeA.2019.8802212.

[14] SK. Liao et al. "Satellite-to-ground quantum key distribution." In: *Nature* 549 (2017), pp. 43–47. DOI: 10.1038/nature23655.